

## Role of synaptic delay in organizing the behavior of networks of self-inhibiting neurons

Steve Kunec and Amitabha Bose\*

*Department of Mathematical Sciences, Center for Applied Mathematics and Statistics, New Jersey Institute of Technology,  
Newark, New Jersey 07102*

(Received 30 June 2000; published 25 January 2001)

We consider a pair of mutually coupled inhibitory neurons in which each neuron is also self-inhibitory. We show that the size of the synaptic delay determines the existence and stability of solutions. For small delays, there is no synchronous solution, but a stable antiphase and a stable on-state solution. For long delays, only the synchronous solution is stable. For intermediate delays, either the antiphase or synchronous solutions are stable. In contrast to prior work, for stability of synchrony, we only require the existence of a single slow process.

DOI: 10.1103/PhysRevE.63.021908

PACS number(s): 87.19.La, 05.45.Xt

### I. INTRODUCTION

Networks of inhibitory neurons exist in various parts of the central nervous system. Efforts to determine the functional role of these networks have been complicated by the complex architecture of and the diversity of synaptic interactions within these heterogeneous networks. For this reason, studies of reduced, if somewhat idealized, models are of importance in that they provide insight into the important network interactions. For example, inhibitory neurons have been implicated in synchronizing cells at the  $\gamma$  frequency in the hippocampal and neocortical systems [1]. The dynamics of inhibitory reticularis cells determine whether the thalamus displays spindle or delta sleep rhythms [2,3]. The behavior of interneuron networks has also been suggested to govern the phase precession phenomenon of hippocampal place cells [4].

Prior studies of mutually coupled inhibitory networks have reported that there are two necessary conditions for stability of the synchronous solution: one is a delay to the onset of inhibition, the other is the existence of an intrinsic slow current that determines the length of the neuron's refractory state and a second slow current [5,6,2,7,8]. The required second slow current can be synaptic such as a GABA-B mediated inhibition, or can be intrinsic to the cell such as a sag current [2].

Self-inhibition has been suggested as a possible mechanism for organizing the behavior of taste receptor cells [9,10], of transient cells involved in visual processing in the locust medulla [11] and in the cortical collecting tubule of rats [12]. At a system level, self-inhibition can also arise as a reduction of a more complicated architecture. For example, *LG* neurons are known to presynaptically inhibit excitatory input to them from *MCN1* cells in the lobster stomatogastric ganglion [13]. Presynaptic inhibition is equivalent to self-inhibition. See Fig. 1.

In this paper, we show that two mutually coupled, self-inhibitory neurons can produce stable synchronous oscillations provided only that the onset of inhibition is delayed for sufficiently long and that the refractory state of the neuron is

also sufficiently long; there is no requirement on the existence of a second slow current. We show that the size of the synaptic delay determines the existence and stability of solutions. For small delays, there is no synchronous solution, but a stable antiphase and a stable on-state solution. For larger delays, the antiphase and synchronous solutions are stable. Finally, for very large delays, only the synchronous solution is stable.

Our paper shows how bistability can be achieved for a robust set of parameters. The results suggest ways in which the network can transition between various rhythmic states. We also provide insight into neural mechanisms that modulate characteristics of the solutions such as the basin of attraction of solutions.

The paper is organized as follows. In Sec. II, we state our modeling equations and assumptions. Here we discuss how to use geometric singular perturbation theory to analyze our model. In Sec. III, we discuss the existence and stability of solutions as a function of the synaptic delay. In Sec. IV, we show how the solutions depend on other parameters of the equations. We also discuss the robustness of the synchronous solution to synaptic and intrinsic heterogeneities. Numerical simulations are provided. Section V is a discussion.

### II. MODEL

We use biophysical conductance based equations to model the cells and the synapses between them. These equa-

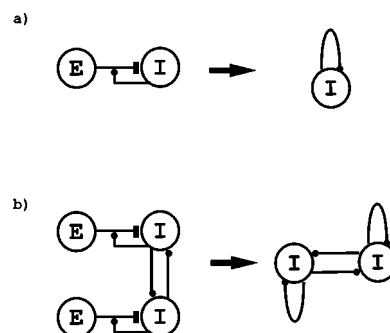


FIG. 1. (a) Equivalence of an excitatory-inhibitory pair with presynaptic inhibition to a single cell with self-inhibition. (b) Equivalence of a network of mutually coupled cells with presynaptic inhibition to a two cell network with mutual and self-inhibition. Dots denote inhibition and bars denote excitation.

\*Email address: bose@m.njit.edu

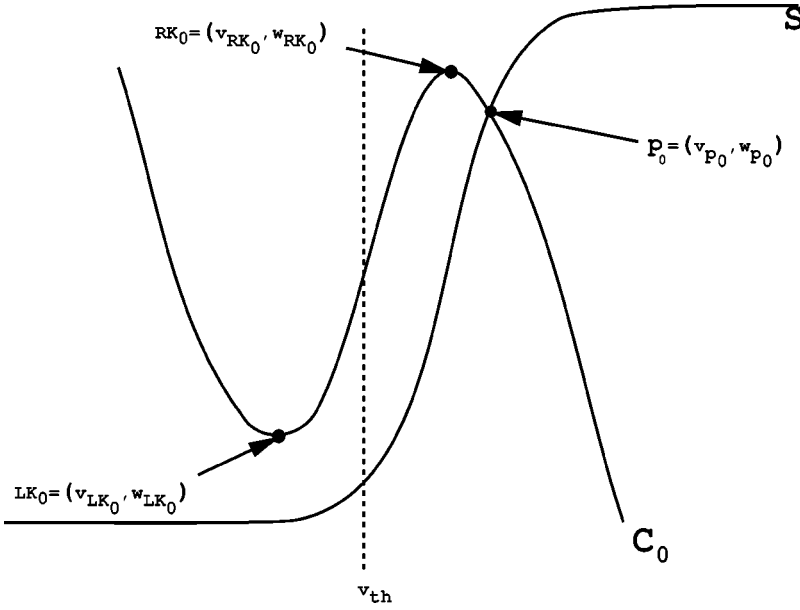


FIG. 2. The nullclines for an isolated inhibitory neuron without self-coupling.

tions can be written compactly in a general form in which the exact details of the equations are less important than the geometric shape of the nullclines of the equations. The equations for an isolated inhibitory cell without self-coupling are

$$\begin{aligned} \epsilon \frac{dv}{dt} &= f(v, w), \\ \frac{dw}{dt} &= [w_\infty(v) - w] / \tau_\infty(v), \end{aligned} \quad (2.1)$$

where  $\epsilon \ll 1$  is the singular perturbation parameter. The  $v$  nullcline is the curve  $C_0 = \{(v, w) : f(v, w) = 0\}$  and is cubic in shape. We let  $LK_0 \equiv (v_{LK_0}, w_{LK_0})$  denote the local minima (also called the left knee) of  $C_0$  and let  $RK_0 \equiv (v_{RK_0}, w_{RK_0})$  denote the local maxima (right knee) of  $C_0$ . The  $w$  nullcline is the curve  $S = \{(v, w) : w_\infty - w = 0\}$  and is a nondecreasing sigmoid. We take

$$w_\infty(v) = \begin{cases} 0 & v < v_a \\ 1 & v > v_b \end{cases} \quad (2.2)$$

for some  $v_{LK_0} < v_a < v_{RK_0} < v_b$ . The functions  $f$  and  $g$  satisfy the following requirements:  $f > 0$  ( $f < 0$ ) below (above)  $C_0$ , and  $g > 0$  ( $g < 0$ ) below (above)  $S$ . The nonlinearity  $f$  contains various ionic currents that are intrinsic to the cell. The nonlinearity  $w_\infty - w$  controls the opening and closing of a potassium channel associated with the cell. See the Appendix for equations.

The function  $\tau_\infty(v)$  is given by

$$\tau_\infty(v) = \begin{cases} \tau_L & v < v_{th} \\ \tau_R & v \geq v_{th} \end{cases}, \quad (2.3)$$

where  $v_{th}$  is a predetermined activity threshold located between the knees of  $C_0$ . The time constants  $\tau_L$  and  $\tau_R$  of the silent and active states are both  $\mathcal{O}(1)$  with respect to  $\epsilon$ . We

assume that  $S$  intersects  $C_0$  on the right branch of  $C_0$  near  $RK_0$  at a point  $p_0 \equiv (v_{p_0}, w_{p_0})$ . See Fig. 2.

Cells communicate at synapses, whereby the ‘‘transmitting’’ or presynaptic cell sends a synaptic current causing either an increase or decrease in the voltage of the ‘‘receiving’’ or postsynaptic cell. The synaptic currents are modeled by adding a term to the right-hand side of the  $v'$  equation for each cell. There are two types of inhibition in our model: self and mutual, both of which act with a delay of time  $\tau$ . The equations for the two coupled cells with mutual and self-inhibition are for  $i = 1, 2$   $i \neq j$ .

$$\begin{aligned} \epsilon \frac{dv_i}{dt} &= f(v_i, w_i) - g_{syn} s_i(t - \tau) [v_i - E_{syn}] \\ &\quad - g_{syn} s_j(t - \tau) [v_i - E_{syn}], \\ \frac{dw_i}{dt} &= [w_\infty(v_i) - w_i] / \tau_\infty(v_i), \\ \epsilon \frac{ds_i}{dt} &= \alpha [1 - s_i] H(v_i - v_{th}) - \beta s_i H(v_{th} - v_i), \\ \epsilon \frac{ds_j}{dt} &= \alpha [1 - s_j] H(v_j - v_{th}) - \beta s_j H(v_{th} - v_j). \end{aligned} \quad (2.4)$$

The  $i$  terms represent self-inhibition, while the  $j$  terms represent mutual inhibition.  $g_{syn}$  is the maximal synaptic conductance.  $E_{syn}$  is the synaptic resting potential. Since the synapses are inhibitory, the reversal potential is less than the cells' voltages,  $v_i - E_{syn} > 0$ .  $s_i$  and  $s_j$  are the synaptic input functions.  $H$  is the Heaviside function and  $v_{th}$  is the synaptic threshold.  $\alpha$  is the synaptic rise and  $\beta$  is the synaptic decay rate constant. We assume that  $\alpha$  and  $\beta$  are both  $\mathcal{O}(1)$  with respect to  $\epsilon$ . Thus the inhibition turns on and off fast like a GABA-A mediated inhibition. Therefore only the variable  $w_i$

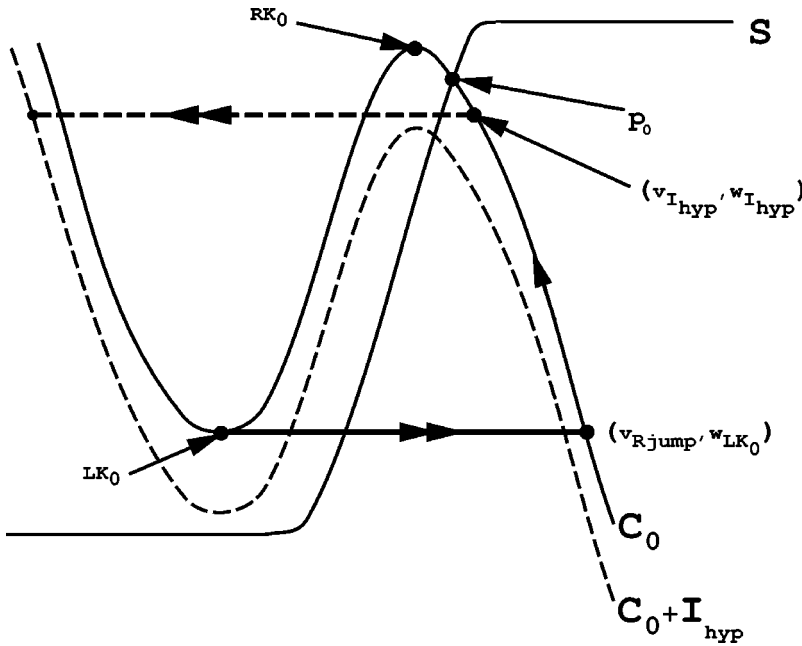


FIG. 3. Trajectories of an isolated inhibitory neuron. The trajectory for the neuron without self-coupling consists of the solid curve connecting  $LK_0$  to  $(v_{Rjump}, w_{LK_0})$  and the solid curve connecting  $(v_{Rjump}, w_{LK_0})$  to  $p_0$ . The dashed portion of the figure represents the changes made to the trajectory of the neuron when a hyperpolarizing current is injected when the cell is at the point  $(v_{Ihyp}, w_{Ihyp})$ . Two arrows denote fast jumps which are solutions of Eq. (2.6), and one arrow denotes slow flows, which are solutions of Eq. (2.5).

evolves slowly in Eq. (2.4) corresponding to the single slow process, which determines the refractory time of the cells.

#### A. Singular solutions

We use geometric singular perturbation theory to construct solutions of Eq. (2.4). This involves using the smallness of the parameter  $\epsilon$  to define reduced fast and slow equations. Solutions to these equations are pieced together to form a so-called singular solution. For the types of equations with which we deal, the existence and stability of the singular solution is sufficient to imply existence and stability of the actual solution to Eq. (2.4) for  $\epsilon$  sufficiently small [14].

It is instructive to first construct the singular solution for a single neuron, without self-coupling. Setting  $\epsilon=0$  in Eq. (2.1), we obtain the slow equations

$$0 = f(v, w), \quad (2.5)$$

$$\frac{dw}{dt} = [w_\infty(v) - w] / \tau_\infty(v).$$

The fast equations are obtained by letting  $\xi = t/\epsilon$  in Eq. (2.1) and then setting  $\epsilon=0$

$$\frac{dv}{d\xi} = f(v, w), \quad (2.6)$$

$$\frac{dw}{d\xi} = 0.$$

Equation (2.5) defines a one-dimensional system where the cell is constrained to move on the cubic  $C_0$ . Its rate of movement is governed by the second equation of Eq. (2.5). When the cell reaches either  $LK_0$  or  $RK_0$ , it makes a fast jump to

the opposite branch using Eq. (2.6). In Eq. (2.6),  $w$  acts like a parameter. The fast system now reduces to a one-dimensional equation

$$\frac{dv}{d\xi} = f(v, \hat{w}), \quad (2.7)$$

where  $\hat{w}$  is constant. As  $\hat{w}$  varies, the critical points of this equation trace out the cubic nullcline  $C_0$ .

The singular orbit of interest is one that leads to the neuron becoming trapped in a so-called on-state. Suppose at  $t=0$ , the cell starts in the silent state at  $LK_0$  on  $C_0$ . Then under Eq. (2.6), the cell will jump to the active state to the right branch of  $C_0$  instantaneously with respect to the slow time  $t$ . The cell then travels up the right branch of  $C_0$  under Eq. (2.5). The stable fixed point  $p_0$  will then attract the cell causing it to become trapped at this high-voltage fixed point. We interpret this solution to represent tonic firing of spikes of a bursting neuron.

The isolated cell can be made to oscillate by adding an appropriate hyperpolarizing current. The effect of such a current is to lower the cubic  $C_0$  in the phase plane; see Fig. 3. Thus if the cell is in a neighborhood of  $p_0$  and negative current is injected, the cell will jump back to the left branch of  $C_0$ . Thus for a cell to jump between active and silent states, it must either reach the knee of a cubic, or receive an appropriately timed dose of inhibition. Notice that a cell with self-inhibition can oscillate if there is a sufficiently long delay to the onset of inhibition.

We now consider the coupled system of reduced fast and slow equations. The fast equations are obtained from Eq. (2.4) by substituting  $\xi = t/\epsilon$  and then setting  $\epsilon$  to 0.

$$\begin{aligned} \frac{dv_i}{d\xi} = & f(v_i, w_i) - g_{syn} s_i(-\tau) [v_i - E_{syn}] \\ & - g_{syn} s_j(-\tau) [v_i - E_{syn}], \end{aligned}$$

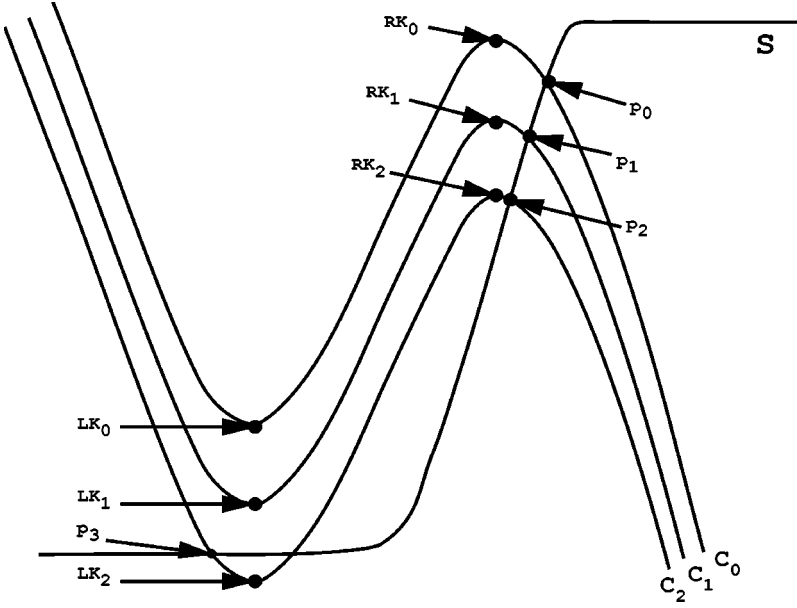


FIG. 4. The three cubic nullclines corresponding to different levels of inhibition.

$$\frac{dw_i}{d\xi} = 0,$$

$$\frac{ds_i}{d\xi} = \alpha[1 - s_i]H(v_i - v_{th}) - \beta s_i H(v_{th} - v_i), \quad (2.8)$$

$$\frac{ds_j}{d\xi} = \alpha[1 - s_j]H(v_j - v_{th}) - \beta s_j H(v_{th} - v_j).$$

The slow equations are obtained directly from Eq. (2.4) by setting  $\epsilon = 0$ .

$$0 = f(v_i, w_i) - g_{syn} s_i (t - \tau) [v_i - E_{syn}] - g_{syn} s_j (t - \tau) [v_i - E_{syn}],$$

$$\frac{dw_i}{dt} = [w_\infty(v_i) - w_i] / \tau_\infty(v_i), \quad (2.9)$$

$$0 = \alpha[1 - s_i]H(v_i - v_{th}) - \beta s_i H(v_{th} - v_i),$$

$$0 = \alpha[1 - s_j]H(v_j - v_{th}) - \beta s_j H(v_{th} - v_j).$$

As with Eq. (2.7), the  $v_i$  equation of Eq. (2.8) can be represented as

$$\frac{dv_i}{d\xi} = F(v_i, \hat{w}, s_i, s_j) \quad (2.10)$$

for a constant  $\hat{w}$ . Notice this equation depends on the values of  $s_i$  and  $s_j$ . As a result, there are two new cubics to consider. They are  $C_1 = \{(v, w, s_i, s_j) : F(v, w, 1, 0) = 0 \text{ or } F(v, w, 0, 1) = 0\}$  and  $C_2 = \{(v, w, s_i, s_j) : F(v, w, 1, 1) = 0\}$ . The cubic  $C_1$  corresponds to the lowered cubic which results from either the self- or mutual inhibition and  $C_2$  represents the lowered cubic that results from both of these inhibitions. The amount that these cubics are lowered is dependent mostly on the strength of the inhibition and is governed

by  $g_{syn}$ . We shall refer to the left and right knees of these cubics by  $LK_i$  and  $RK_i$ , for  $i = 1, 2$ . The intersection of the right branches of the lowered cubics with the sigmoid  $S$  defines two new fixed points  $p_1$  and  $p_2$ . We assume that  $w_{p_2} < w_{RK_2} < w_{p_1} < w_{RK_1} < w_{p_0}$ . We also assume that  $S$  intersects  $C_2$  along its left branch at a point  $p_3$ ; see Fig. 4. Also, since  $w_\infty = 0$  near the left branches of these cubics, the rate of  $w$  evolution on the left branches is independent of which cubic a cell may lie on. This is not the case for the right branches.

## B. Main result

We shall establish the existence and stability of three different types of solutions. The first is the on-state solution, where both cells are trapped at a high-voltage fixed point. The second is a synchronous periodic orbit. The third is an antiphase solution in which when one cell jumps to the active phase, the other cell jumps down to the silent phase after a delay of  $\tau$ . We shall always work in the  $\epsilon = 0$  singular limit since results of Ref. [14] imply that the singular solutions of interest perturb to yield actual solutions for the full  $\epsilon$  small problem.

Our goal is to study this problem with all parameters fixed and to see how the existence and stability of solutions depends on the delay  $\tau$ . To this end, we will show that for a fixed  $\tau$ , at most two of the above-mentioned solutions can be stable. We will provide conditions on the basin of attraction of each of these solutions. Depending on the value of the parameters, the model that we consider can display incredibly complicated and diverse dynamical behavior. Thus to give a precise statement of the results, we shall make a few assumptions. Later, we will show how some of the results are affected by changing assumptions.

Let  $\tau_*$  be the time it takes a cell to travel on the right branch of  $C_0$  from  $w_{LK_0}$  to  $w_{RK_2}$ , and  $T_l$  be the time on the left branch of  $C_0$  between these two points; see Fig. 5. Let  $\tau^*$  be the time on the right branch of  $C_0$  from  $w_{LK_0}$  to  $w_{RK_1}$ . Let  $T^R$  be the time it takes a cell to travel on the right branch of

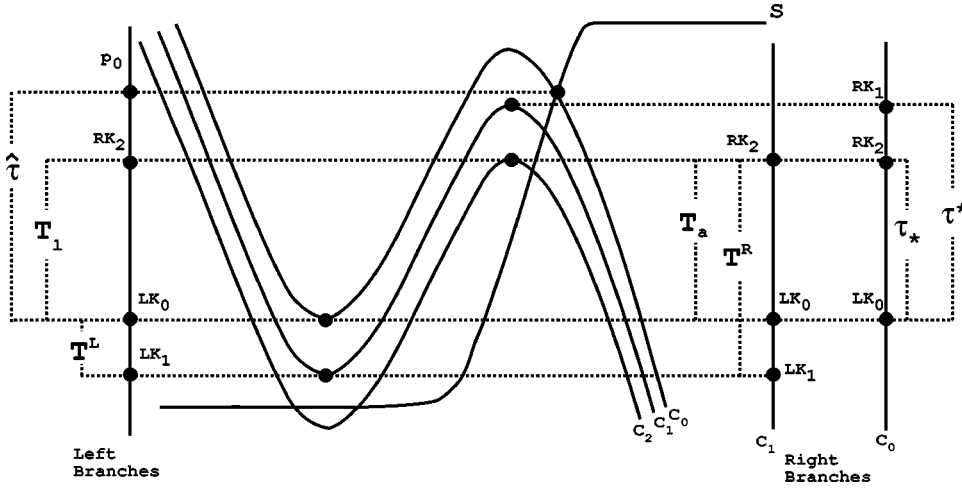


FIG. 5. Time lengths of evolution between relevant points on various cubic nullclines. For clarity, the times have been projected (to the right and left) onto simplified versions of the branches of the nullclines.

$C_1$  from  $w_{LK_1}$  to  $w_{RK_2}$ ,  $T_a$  the time on the right branch of  $C_1$  from  $w_{LK_0}$  to  $w_{RK_2}$ ,  $\hat{\tau}$  be the time it takes to travel on the left branch of  $C_0$  from  $w_{p_0}$  to  $w_{LK_0}$ , and  $T^L$  be the time it takes to travel on the left branch of  $C_1$  from  $w_{LK_0}$  to  $w_{LK_1}$ . We make the following two assumptions:

$$(A1) \tau^* < T_a < T_l \quad (A2) T^R < \hat{\tau} < T^L.$$

The crux of these assumptions is that evolution in the silent state of the neuron is slower than in the active state. To state the main theorem, we shall restrict the set of initial conditions to the interval  $[0, \hat{\tau}]$ . This is sufficient since a given cell must jump down from the active state with a  $w$  value that is less than  $w_{p_0}$ .

#### Theorem 1

If  $\Delta t_0 \in [0, \hat{\tau}]$ , then there exists  $\bar{\tau} \in (\tau^*, \hat{\tau})$  such that

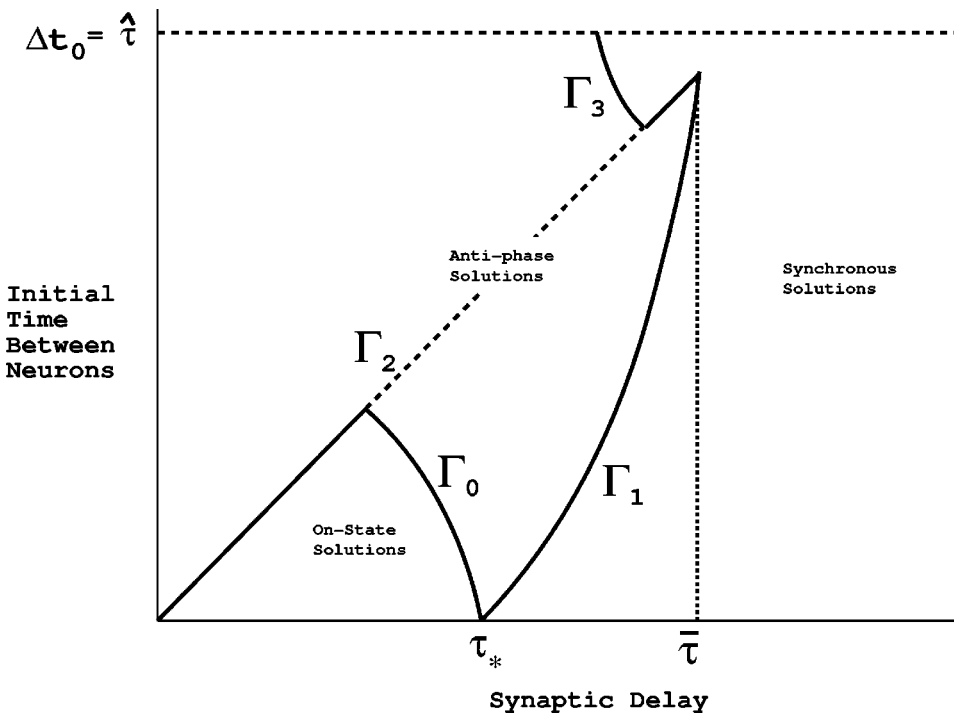


FIG. 6. The bifurcation diagram relating the delay to the basin of attraction of each type of solution. At most two solutions can be stable for the same delay. The curves  $\Gamma_i$ ,  $i=0, \dots, 3$  separate different solution regimes. The diagonal  $\Gamma_2$  consists of a solid and a dashed portion. The dashed portion separates initial conditions that approach the anti-phase solution in different ways.

- (i) if  $\tau < \tau_*$ , there exists both a stable on-state and a stable antiphase solution.
- (ii) if  $\tau_* \leq \tau < \bar{\tau}$ , there exists both a stable synchronous and a stable antiphase solution.
- (iii) if  $\bar{\tau} < \tau$ , then there exists only a stable synchronous orbit.

Each of the stable solutions has a corresponding basin of attraction, which we shall identify in the analysis below; Fig. 6 shows the bifurcation diagram.

### III. EXISTENCE AND STABILITY OF SOLUTIONS

Establishing existence and stability of the on-state and synchronous solution is straight forward. Doing the same for the antiphase solution is a bit more involved. For the on-state and synchronous solution, we prove stability by directly showing that cells that start nearby to either of these solutions approach them as time evolves. For the antiphase solu-

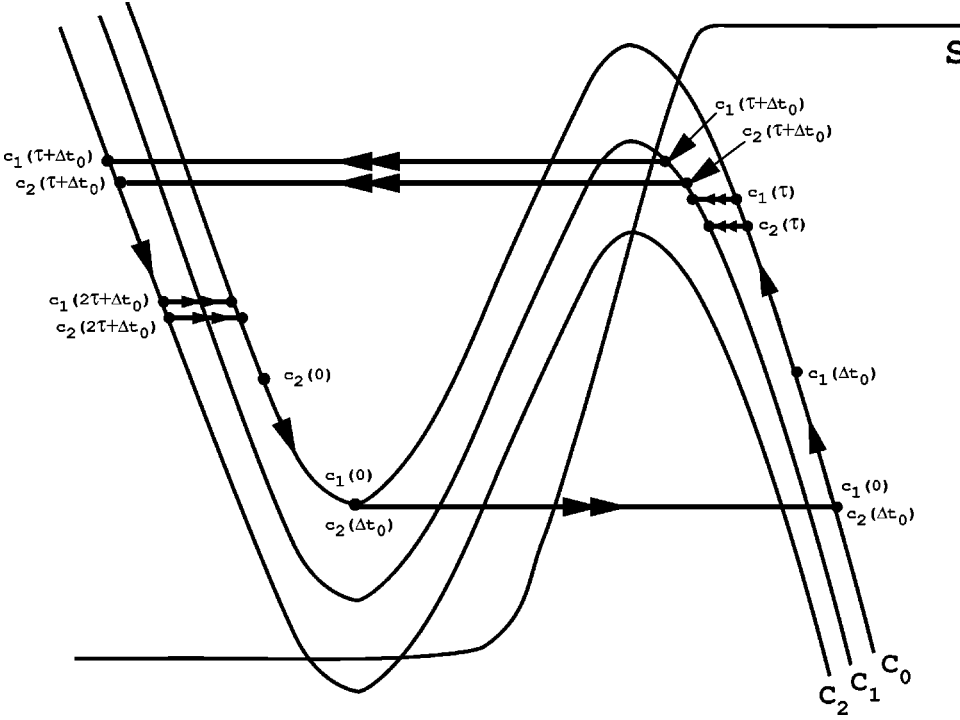


FIG. 7. The path of two cells in the phase plane as they approach synchrony, for intermediate delays. The notation  $c_i(t)$  denotes the position of cell  $i$  at time  $t$ .  $\Delta t_0$  denotes the initial time distance between cells at  $t=0$ .

tion, stability is established by showing that the solution is obtained as a fixed point of a relevant contraction mapping.

#### A. The on-state solution for short delays

We first discuss the existence of the on-state solution. Suppose both neurons start at  $LK_0$  and  $\tau < \tau_*$ . At  $t=0$ , both cells jump to the active state. Due to the delay, the inhibition will not be felt for  $\tau$  time, so both cells jump to the right branch of  $C_0$  and travel up. After time  $\tau$ , both the self- and mutual inhibition turn on. Since  $\tau < \tau_*$ ,  $w_1(\tau) = w_2(\tau) < w_{RK_2}$  and are thus not above the right knee of  $C_2$  when the inhibition is felt. As a result, both will jump to the right branch of  $C_2$  and become trapped at  $p_2$ .

To prove the stability, we start with the cells a fixed distance apart such that  $\Delta t_0 < \tau$ . At  $t=0$ ,  $c_1$  jumps to the right branch of  $C_0$ . Since  $\tau < \tau_*$ ,  $w_1(\tau) < w_{RK_2}$ . Since  $\Delta t_0 < \tau$ ,  $c_2$  reaches  $LK_0$  and jumps before the inhibition due to  $c_1$  turns on. When the inhibition due to  $c_1$  activates, both cells jump back to the right branch of  $C_1$ . The inhibition due to  $c_2$  will come after another  $\Delta t_0$  time. If  $w_1(\tau + \Delta t_0) < w_{RK_2}$ , then both cells will become trapped by  $p_2$ . If  $w_1(\tau + \Delta t_0) > w_{RK_2}$  and  $w_2(\tau + \Delta t_0) < w_{RK_2}$ , the cells will approach an antiphase solution; and if  $w_2(\tau + \Delta t_0) > w_{RK_2}$  the cells will approach a synchronous solution. Both of these solutions are discussed below. The curved labeled  $\Gamma_0$  in Fig. 6 represents the case when  $w_1(\tau + \Delta t_0) = w_{RK_2}$ . This curve is one boundary between the antiphase and on-state solution regions. The curve  $\Gamma_1$  represents the case when  $w_2(\tau + \Delta t_0) = w_{RK_2}$ . This curve is one boundary between the antiphase and synchronous solution regions.

#### B. The synchronous solution for intermediate delays

We continue by discussing the existence of the synchronous solution. Suppose both cells start at  $LK_0$  jump to the right branch of  $C_0$ . There, they travel up that branch until inhibition turns on, after time  $\tau$ . For the synchronous solution to exist, it is necessary for  $\tau \geq \tau_*$ . In other words, both cells need to travel up the the right branch of  $C_0$  above  $RK_2$  before the self- and mutual inhibition is felt. At  $t=\tau$ , the cells can then jump to the left branch of  $C_2$ . At  $t=2\tau$ , the cells return to the left branch of  $C_0$  and the process repeats.

Next, we discuss the stability of the synchronous solution. Suppose first that  $\tau < \tau_*$ . We start  $c_1$  at  $LK_0$  and  $c_2$  at some time distance  $\Delta t_0$ , above  $c_1$  on the left branch of  $C_0$  such that  $\Delta t_0 < \tau$ . At  $t=0$ ,  $c_1$  jumps to the right branch of  $C_0$ . After time  $\Delta t_0$ ,  $c_2$  will jump to the right branch of  $C_0$ .

Now both cells travel up the right branch of  $C_0$ . As they get closer to  $p_0$ , the neurons move closer together in Euclidean distance. Note, however, the cells remain the same time distance apart. This is because both cells adhere to the same differential equations and have followed the same trajectory.

After time  $\tau$ , the inhibition due to  $c_1$  crossing the synaptic threshold, will turn on. Since  $\tau < \tau_*$ , both cells jump left to the right branch of  $C_1$ . For the next  $\Delta t_0$  time, both cells travel toward  $p_1$  as Euclidean compression continues to occur. When the second inhibition turns on, since  $\tau > \tau_*$ , if  $\Delta t_0$  is sufficiently small, then both cells jump to the left branch of  $C_2$ , see Fig. 7. It is of fundamental importance that the cells jump down to the silent state at the same time because this causes a compression in time between cells due to fast threshold modulation [15]. This occurs because the vertical speed on the right branch of  $C_1$  at the jump down point is less than the vertical speed at the jump on point on the left branch of  $C_2$ . Since the cells remain the same Euclidean dis-

tance apart before and after the jump, but the speed increases after the jump, the time distance between the cells must decrease. Let the new time distance be denoted by  $\Delta t_1 < \Delta t_0$ . Note that after the jump,  $c_2$  is now the leading cell, being below  $c_1$  on the left branch of  $\mathcal{C}_2$ .

Both cells now travel down the left branch of  $\mathcal{C}_2$ .  $\tau$  time after the cells have jumped down, inhibition turns off for both cells, since they jumped down simultaneously. Since  $\tau < \tau^*$ , by assumption (A1), the cells then return to the left branch of  $\mathcal{C}_0$  above  $LK_0$ .

There is no time compression expansion as the cells jump between the left branches of  $\mathcal{C}_2$  and  $\mathcal{C}_0$  since the rate on the left branches is independent of cubic. Thus when  $c_2$  reaches  $LK_0$ , the time between cells is  $\Delta t_1$ , which is less than the original time apart. Thus the cells approach synchrony.

The rate at which they synchronize is most strongly governed by the amount of time compression across the down jump. This amount is controlled by the relative speeds on each branch and the total amount of Euclidean compression the cells undergo in a neighborhood of the fixed points  $p_0$  and  $p_1$ . We note that the existence of the fixed points is not necessary for the stability of the intermediate delay synchronous solution. There would still be Euclidean compression without the fixed points, but it would not be as strong. Thus the fixed points increase the rate at which the cells synchronize. Later we show that they are important for the long delay synchrony.

In Sec. III D, we will discuss the existence and stability of the synchronous solution for  $\tau > \tau^*$ .

### C. The antiphase solution for short and intermediate delays

We next show that a stable antiphase solution exists. We define an antiphase solution as being an oscillation in which when one cell becomes active, the other cell becomes inactive after a delay of  $\tau$ .

As usual, let  $c_1$  start at  $LK_0$  and  $c_2$  start on the left branch of  $\mathcal{C}_0$ , such that they are  $\Delta t_0$  apart in time. There are two ways that the cells will approach an antiphase solution:

(1) If  $\tau < \Delta t_0$ , then  $c_2$  does not reach  $LK_0$  before the inhibition due to  $c_1$  is felt and will jump back to the left branch of  $\mathcal{C}_1$  at  $t = \tau$ . By assumption (A2),  $c_1$  rises above  $RK_2$  before  $c_2$  reaches  $LK_1$ . Assume that  $\tau < \tau^*$  so that  $w_1(\tau) < w_{RK_1}$ . So when the first inhibition is felt,  $c_1$  will jump left onto the right branch of  $\mathcal{C}_1$ , above  $RK_2$  but below  $RK_1$  and become trapped by  $p_1$ . In the meantime,  $c_2$  travels down the left branch of  $\mathcal{C}_1$  until it reaches  $LK_1$ , and jumps to the right branch of  $\mathcal{C}_1$ . After time  $\tau$ , the inhibition due to  $c_2$  causes  $c_1$  to jump down to the left branch of  $\mathcal{C}_2$  and  $c_2$  to jump back to the right branch of this cubic. After another time  $\tau$  by assumption (A1),  $c_1$  jumps to the left branch of  $\mathcal{C}_1$  and  $c_2$  jumps to the right branch of this cubic. The curve  $\Gamma_2$  in Fig. 6 is the diagonal  $\Delta t_0 = \tau$ . Therefore initial conditions that fall into this case lie above the curve  $\Gamma_2$ .

(2) If  $\tau > \Delta t_0$ , then  $c_2$  is able to reach  $LK_0$  and jump right, before the inhibition due to  $c_1$  is felt. At  $t = \tau$ , both cells jump left to the right branch of  $\mathcal{C}_1$ . The second inhibition, due to  $c_2$ , arrives  $\Delta t_0$  later. If  $\tau < \tau^*$  and the initial conditions are such that  $c_2$  does not rise vertically above  $RK_2$  by

the onset of the next inhibition, the overlapping inhibitions will cause  $c_1$  to jump onto the left branch of  $\mathcal{C}_2$ , and  $c_2$  will jump onto the right branch of  $\mathcal{C}_2$ . From there,  $c_2$  will travel up towards  $p_2$ , while  $c_1$  will travel down towards  $LK_2$ . After time  $\tau$ ,  $c_1$ 's inhibition turns off, and by assumption (A1),  $c_1$  jumps onto the left branch of  $\mathcal{C}_1$  and  $c_2$  jumps onto the right branch of  $\mathcal{C}_1$ . Now,  $c_1$  travels down until it reaches  $LK_1$  and  $c_2$  travels up towards  $p_1$ . This case corresponds to the region of Fig. 6, which is bounded by the curves  $\Gamma_0$ ,  $\Gamma_1$ , and  $\Gamma_2$ .

In both scenarios above, the cells eventually evolve to the following configuration. One cell is at  $LK_1$  (without loss of generality, call this cell  $c_1$ ). Another cell is located on the right branch of  $\mathcal{C}_1$  (without loss of generality call this cell  $c_2$ ). We now take this to be the setup at  $t = 0$ .

Let  $B$  be a set of initial  $w$  positions of  $c_2$  on the right branch of  $\mathcal{C}_1$ , defined as follows. The set  $B$  will include all points from  $w_{p_1}$  down to the point that is  $\tau$  time below  $RK_2$ . Let the  $w$ -value of this point be denoted by  $\tilde{w}$ . Therefore, the set  $B = (\tilde{w}, w_{p_1})$ .

At  $t = 0$ ,  $c_1$  jumps to the right branch of  $\mathcal{C}_1$  and  $c_2$  moves up that branch towards  $p_1$ . After  $\tau$  time, inhibition due to  $c_1$  turns on. Since  $\tau < \tau^*$  and  $T_a < T^R$ , by assumption (A1),  $c_1$  has not risen above  $RK_2$ , and so it jumps to the right branch of  $\mathcal{C}_2$ .  $c_2$  jumps to the left branch of  $\mathcal{C}_2$  because after time  $\tau$ , it has definitely risen above  $RK_2$  and is able to jump left. After another time  $\tau$ , the inhibition due to  $c_2$  turns off, since it crossed the synaptic threshold while jumping to the left. By Eq. (A1),  $c_1$  now jumps to the right branch of  $\mathcal{C}_1$  while  $c_2$  jumps to the left branch of  $\mathcal{C}_1$ . Let  $T_2$  be the time it takes to move from  $c_2$ 's current position down to  $LK_1$ ; see Fig. 8.

To prove existence of the antiphase solution, we show that there exists a mapping of the set  $B$  into itself. Whenever a cell reaches  $LK_1$ , the map will record the position of the other cell on the right branch of  $\mathcal{C}_1$ .

When a cell is on the left branch of any cubic,  $w_\infty(v) = 0$ . Therefore, the rate of  $w$  evolution is governed by

$$\frac{dw}{dt} = -\frac{w}{\tau_L}. \quad (3.1)$$

Solving (3.1) for time, we obtain

$$t = \tau_L \ln\left(\frac{w_0^L}{w}\right), \quad (3.2)$$

which is the time it takes to travel from some initial height  $w_0^L$  on the left branch of a cubic down to a height of  $w$ .

On the right branch of a cubic, the situation is more delicate. It is possible that a cell is below the part of the sigmoid that is not constant with respect to  $v$ , i.e. the sloping part of the sigmoid. In this case, we must consider the full  $w$  differential equation, or at least a good approximation of it.

For  $v \in (v_a, v_b)$ , let

$$\frac{dw}{dt} = \frac{1}{\tau_R}(a_1 v - b_1 - w), \quad (3.3)$$

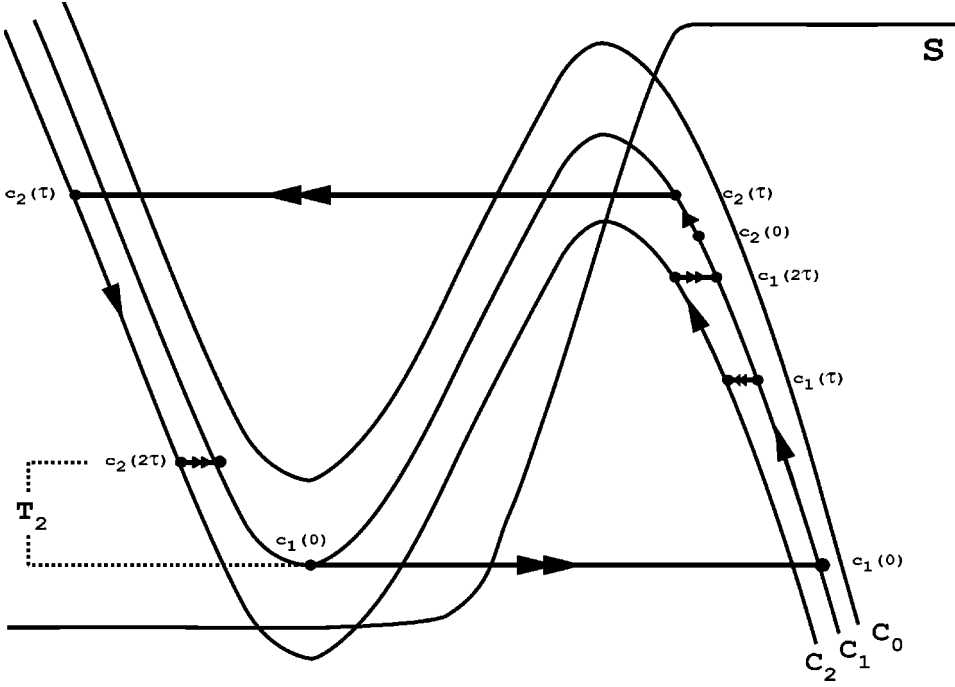


FIG. 8. The path of two cells in the antiphase solution in the phase plane. For the antiphase solution, the time from  $c_1(2\tau)$  to the position  $c_2(0)$  is exactly  $T_2$ .

where the sigmoid  $w_\infty(v)$  is approximated by the line  $a_1v - b_1$ . We're assuming that while the neuron is on the right branch of  $\mathcal{C}_1$ , it is always below this sloping part of the sigmoid (which we are approximating with a line). If this is not the case, and for some amount of time the neuron is below the horizontal portion of the sigmoid, the time can easily be calculated, since  $w_\infty(v) = 1$ .

To eliminate  $v$  in Eq. (3.3), we also approximate the right branch of  $\mathcal{C}_1$  with a line  $w = -a_2v + b_2$ .

Equation (3.3) now becomes

$$\frac{dw}{dt} = \frac{1}{\tau_R} \left[ a_1 \left( \frac{w - b_2}{-a_2} \right) - b_1 - w \right], \quad (3.4)$$

which can be simplified to

$$\frac{dw}{dt} = \frac{1}{\tau_R} (D - Ew), \quad (3.5)$$

where  $E = a_1/a_2 + 1$  and  $D = a_1b_2/a_2 - b_1$ . The constants  $a_1$ ,  $b_1$ ,  $a_2$ , and  $b_2$  are all positive numbers. Therefore,  $E$  is also positive. Note that  $D$  must be positive as well. We know this because  $dw/dt > 0$  on the right branch of a cubic. This also implies that  $Ew$  must be less than  $D$  as long as the cell is below  $p_1$ , whose  $w$  coordinate is  $D/E$ .

Equation (3.5) can be solved for  $w$  while on the right branch of a cubic. We obtain

$$w(t) = w_0^R e^{-Et/\tau_R} + \frac{D}{E} (1 - e^{-Et/\tau_R}), \quad (3.6)$$

where  $w_0^R$  is the initial position of the cell on the right branch of the cubic. Using the initial conditions defined earlier, after time  $\tau$ , the  $w$  value of  $c_2$  on the right branch of  $\mathcal{C}_1$  is given by

$$w_2(\tau) = w_2(0) e^{-E\tau/\tau_R} + \frac{D}{E} (1 - e^{-E\tau/\tau_R}). \quad (3.7)$$

At  $t = \tau$ , the inhibition from  $c_1$  activates, causing  $c_2$  to jump down to the left branch of  $\mathcal{C}_2$ . At  $t = 2\tau$ ,  $c_2$  jumps to the left branch of  $\mathcal{C}_1$  and then travels to  $LK_1$ . Using Eq. (3.2) for the time on the left branch of a cubic, we obtain an expression for  $T_2$  (see Fig. 8) which is

$$T_2 = \tau_L \ln \left( \frac{w_2(\tau)}{w_{LK_1}} \right) - \tau. \quad (3.8)$$

If we substitute  $T_2$  into Eq. (3.6), with an initial position of  $w_1(2\tau)$ , we obtain an equation for the position of  $c_1$  after  $c_2$  has reached the left knee of  $\mathcal{C}_1$ . The map is defined by

$$M_A(w_2) = \frac{D}{E} + \left( w_1(2\tau) - \frac{D}{E} \right) e^{E\tau/\tau_R} \left( \frac{w_2(\tau)}{w_{LK_1}} \right)^{-E\tau_L/\tau_R}. \quad (3.9)$$

Substituting Eq. (3.7) into Eq. (3.9) yields

$$M_A(w_2) = \frac{D}{E} + \left( w_1(2\tau) - \frac{D}{E} \right) \cdot e^{E\tau/\tau_R} \times \left( \frac{w_2(0) e^{-E\tau/\tau_R} + \frac{D}{E} (1 - e^{-E\tau/\tau_R})}{w_{LK_1}} \right)^{-E\tau_L/\tau_R}. \quad (3.10)$$

Now, we can show that  $M_A$  maps  $B$  into itself. First, consider  $w_2(0) = w_{p_1}$  corresponding to an infinite time distance from the cell at the left knee of  $\mathcal{C}_1$ . By substituting  $D/E$  into Eq. (3.10), we see that the term  $[w_1(2\tau) - D/E]$  is

negative, since  $w_1(2\tau)$  is always less than the critical point located at  $w = D/E$ , and every other term is positive. Therefore,  $w_{p_1}$  is mapped to a point lower than itself.

Next we check that at the other end point of  $B$ , that  $M_A(\tilde{w}) > \tilde{w}$ . Here we use the assumption (A2) that  $T^R < T^L$ . Since  $T_2 > T^L$  and the time it takes to go from  $w_{LK_1}$  to  $\tilde{w}$  is less than  $T^R$ , this ensures that the point  $\tilde{w}$  will be mapped to a point above itself. Therefore, since  $B$  is mapped into itself, there exists an initial condition within  $B$  which is mapped to itself. This fixed point corresponds to the antiphase solution.

To show local uniqueness and stability of the antiphase solution, we show that  $M_A$  is a contraction mapping of  $B$  into itself. This can be achieved by showing that  $|M'_A(w_2)| < 1$ , where  $'$  denotes derivative with respect to  $w_2(0)$ , for all  $w_2(0) \in B$ . Taking the derivative, we find

$$M'_A(w_2) = \frac{E\tau_L}{\tau_R w_0} \left( \frac{D}{E} - w_1 \right) \times \left[ \frac{w_2 e^{-E\tau/\tau_R} + D/E(1 - e^{-E\tau/\tau_R})}{w_{LK_1}} \right]^{-(E\tau_L/\tau_R + 1)}. \quad (3.11)$$

Notice that the first term is larger than one, but the second and third are less than one. However the first term is algebraic in the ratio  $\tau_L/\tau_R$  while the third term is exponential in this ratio. Thus for  $\tau_L/\tau_R$  sufficiently large, the product can clearly be made less than 1. Note that  $\tau_L/\tau_R > 1$  is consistent with assumptions (A1) and (A2). In this case, the antiphase solution is stable.

#### D. The antiphase and synchronous solution for longer delays

We now show how to extend the analysis to consider delays larger than  $\tau^*$ . Consider for a moment the case where  $\tau = \tau^*$  and  $\Delta t_0 = \tau^* - \delta$ , where  $\delta$  is a small positive number. At  $t=0$ ,  $c_1$  jumps to the right branch of  $C_0$ . At  $t = \tau^* - \delta$ ,  $c_2$  jumps up to the right branch of  $C_0$ . At  $t = \tau^*$ , both cells fall back to the right branch of  $C_1$ . By assumption (A1),  $\tau^* < T_a$ , thus  $w_2(2\tau^* - \delta) < w_{RK_2}$ . This implies that when the inhibition due to  $c_2$  turns on,  $c_1$  will jump down to the silent state to the right branch of  $C_2$ , while  $c_2$  will stay in the active state on the right branch of that cubic. After another time  $\tau$ , both cells jump to  $C_1$ , with  $c_1$  on the left branch and  $c_2$  on the right branch of that cubic. From there, the cells evolve until  $c_1$  reaches  $LK_1$ . This situation has already been analyzed and we know that the cells tend towards the antiphase solution. Thus for  $\tau = \tau^*$  and  $\Delta t_0 = \tau^* - \delta$ , the cells do not synchronize. This implies that at  $\tau = \tau^*$ , the curve  $\Gamma_1$  lies below the curve  $\Gamma_2$ .

Next consider the case  $\Delta t_0 = \hat{\tau}$  and  $\tau = \hat{\tau} - \delta$  for some  $\delta$  positive and small. At  $t=0$ ,  $c_1$  jumps up to the right branch of  $C_0$ . At  $t = \hat{\tau} - \delta$ , by assumptions (A1) and (A2),  $w_1(\hat{\tau} - \delta) > w_{RK_1}$ , while, on the left branch of  $C_0$ ,  $w_2(\hat{\tau} - \delta) > w_{LK_0}$ . Thus both cells jump back to the left branch of  $C_1$ . The cells evolve down  $C_1$  until  $t = 2(\hat{\tau} - \delta)$  when the inhibi-

tion due to  $c_1$  wears off. By assumption (A2),  $c_2$  has not yet reached  $LK_1$ , and by the definition of  $\hat{\tau}$ ,  $w_1(2(\hat{\tau} - \delta))$  is below  $LK_0$ . Thus both cells jump to the right branch of  $C_0$ . Fast threshold modulation [15] causes a compression in time between the cells. Notice that the time on  $C_0$  from  $LK_1$  to  $RK_2$  is less than  $T^R$  since the  $w$  rate on  $C_0$  is faster than on  $C_1$ . Therefore by (A2), since  $T^R < \hat{\tau}$ , the cells are above  $RK_2$  when the self- and mutual inhibitions turn on. Note that this occurs simultaneously since both cells jumped up at the same time. Therefore the cells jump down together. Again because of fast threshold modulation, there is time compression across this jump, and thus the cells synchronize. This result shows that the curve  $\Gamma_2$  does not intersect the line  $\Delta t_0 = \hat{\tau}$ . Therefore, let  $\bar{\tau}$  be the value of  $\tau$  at which  $\Gamma_2$  and  $\Gamma_1$  intersect.

Exactly the same argument as above shows that if  $\tau = \bar{\tau}$  and  $\Delta t_0 = \bar{\tau} + \delta$ , for  $\delta$  sufficiently small and positive, then the cells tend towards the synchronous solution. For the same set of initial conditions, but for sufficiently small delays, we recall that the cells tend towards an antiphase solution. This implies that there exists a curve  $\Gamma_3$ , which lies above  $\Gamma_2$ , which separates the antiphase region from the synchronous region for initial conditions that are a relatively large distance apart.

Finally, we discuss why only the synchronous solution is stable if the delay is sufficiently long. Suppose, for example that  $\tau > \hat{\tau} + T^L$ . If the cells both start near  $LK_0$ , then they jump to the active phase, evolve above  $w_{RK_1}$  and jump down, eventually to  $C_2$  at  $t = \tau + \Delta t_0$ . Now since the delay is so long, both cells are below  $w_{LK_1}$  when the first inhibition wears off. Moreover, until this time, the fixed point  $p_3$  prevents them from jumping up to the active state. Thus the cells jump up to the active state together at  $t = 2\tau$ . Since the cells jump down and up together, as before, they synchronize.

This completes the analysis needed to establish Theorem 1 and the bifurcation diagram shown in Fig. 6.

#### IV. PARAMETER DEPENDENCE AND NUMERICAL SIMULATIONS

In Fig. 9, we show the results of a simulation using model equations based on the Morris-Lecar equations [16]; see the Appendix for equations and parameter values. In the figure, we start the cells with initial conditions which lie above  $\Gamma_2$  in the bifurcation diagram. As is seen, the cells tend towards the antiphase solution. Around  $t = 1200$ , we increased the delay enough so that the cells synchronize. Next, around  $t = 2700$ , we decreased the delay, so that the synchronous orbit disappears and the cells become trapped in the on-state solution.

We next discuss how the solutions depend on various parameters. The existence and stability results do not depend substantially on the size of the coupling  $g_{syn}$ , nor on the fact that the maximal conductances for the self- and mutual coupling are the same. It is required that the inhibitions are strong enough to make  $w_{RK_2} < w_{p_1} < w_{RK_1} < w_{p_0}$ . The size of the inhibition will affect the basin of attraction of the solu-

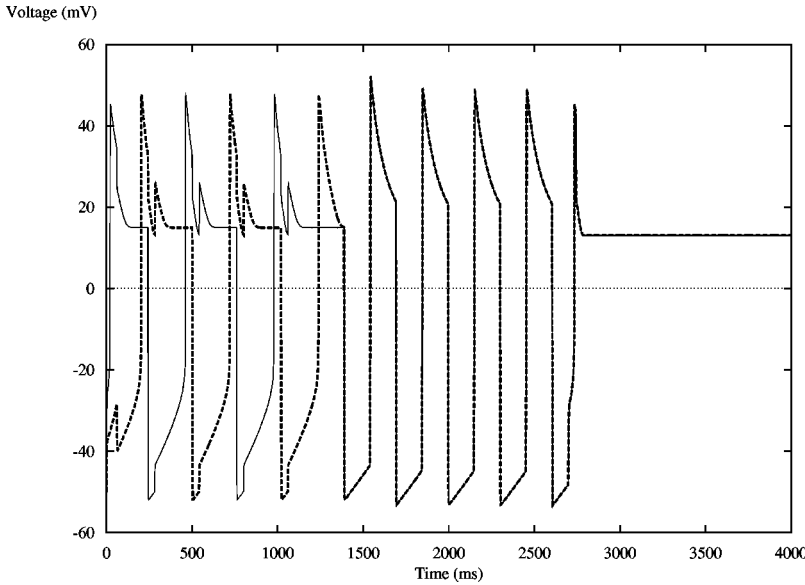


FIG. 9. The effect of changing the synaptic delay. We started the cells in the antiphase regime with  $\tau=40$ . At  $t=1200$ , the delay was increased to  $\tau=150$  and the solution changed from antiphase to synchronous. At  $t=2700$ , the delay was decreased to  $\tau=10$  and the solution changed from synchronous to the on-state.

tions, though. For example, stronger inhibition increases the basin of attraction of the synchronous solution for a fixed delay by making, among other things,  $\tau_*$  smaller. Similarly the rates  $\tau_R$  and  $\tau_L$  also affect the basin of attraction of solutions. A larger  $\tau_R$  means a faster right-hand branch, which also increases the basin of attraction of the synchronous solution by making  $\tau_*$  smaller.

We next show that the synchronous solution persists in the face of different types of heterogeneities. First suppose that the self-inhibitory delay ( $\tau_s$ ) is shorter than the mutual-inhibitory delay ( $\tau_m$ ), but both are larger than  $\tau_*$ . If the cells start close to one another near  $LK_0$ , then the leading cell is the first to jump down from the active state. Thus in the time before the trailing cell feels the mutual inhibition (or self-inhibition from itself), the cells will be moving in opposite directions on opposite branches. The leading cell will be moving down the right branch of  $C_1$  and the trailing cell will be moving up the right branch of  $C_0$ . Thus the  $w$  values of the cells will become closer. If the trailing cell jumps down relatively soon thereafter, the cells will be closer in time. Therefore if the initial conditions are not too far apart and  $\tau_s < \tau_m$  is not too large, the cells will synchronize.

Alternatively, if  $\tau_m < \tau_s$ , then the synchronous solution will still be stable. In this case, the trailing cell will jump down before the leading cell at  $t=\tau_m$ , and there will be a time expansion until the leading cell also jumps down. The trailing cell  $c_2$  will now be below the previously leading cell  $c_1$  on the left branch of  $C_1$ . At some time later, both cells will receive a second amount of inhibition. The time at which this occurs is not important here. The cells will move to the left branch of  $C_2$  and remain in the same relative position,  $c_2$  below  $c_1$ . Eventually, the inhibition will turn off. For sufficiently large delays, both cells will travel down the left branch of  $C_2$  below  $LK_0$ . At time  $2\tau_m$ ,  $c_1$  will lose inhibition and jump right onto the left branch of  $C_1$ , where it will travel down. At time  $\tau_m + \tau_s$ ,  $c_2$  will lose all of its inhibition and jump right onto the right branch of  $C_0$  (this is evident by considering the time when  $c_2$  originally jumped down from the right branch of  $C_0$ ).  $c_2$  will now have time to travel up

the right branch of  $C_0$  before  $c_1$  loses the last of its inhibition at time  $2\tau_s$ . Since  $c_1$  was moving down towards  $LK_1$  and  $c_2$  was moving up the right branch of  $C_0$ , there is time compression. If  $\Delta t_0$  and  $\tau_s - \tau_m$  are not too large, then the cells synchronize.

In both cases above, although the cells do not jump down or up at exactly the same time, they do so in a small time window of one another. Thus the ideas that underlie synchronization through fast threshold modulation still apply to these cases.

Suppose  $\tau_* < \tau_s, \tau_m < \tau_*$ , such that both cells receive the first inhibition between  $RK_1$  and  $RK_2$ . For  $\tau_s < \tau_m$ , the cells move away from synchrony. At time  $\tau_s$ ,  $c_1$  jumps down to the right branch of  $C_1$ .  $c_2$  does the same at time  $\tau_m$  or  $\tau_s + \Delta t_0$ , depending on which is less. Then  $c_2$  jumps left onto the left branch of  $C_2$  at time  $\tau_m$  or  $\tau_s + \Delta t_0$ , depending on which is more. Now,  $c_2$  has time to travel down the left branch of  $C_2$  until  $c_1$  jumps left onto the same branch at time  $\tau_m + \Delta t_0$ . The result is time expansion. Here we are assuming that the delays are sufficiently small so that both cells return to the left branch of  $C_0$  when the inhibition turns off. If the delays are large enough so that both cells are below  $LK_0$ , then the cells may still approach synchrony, as described previously for delays greater than  $\tau_*$ .

For  $\tau_m < \tau_s$ ,  $c_1$  will reach the left branch of  $C_2$  first, in a manner similar to the process in the previous paragraph.  $c_1$  travels down the left branch while  $c_2$  travels up the right branch of  $C_1$  until  $c_2$  jumps left, arriving closer to  $c_1$ . Again, there is time compression. The above results were obtained with up to 5% of heterogeneity between  $\tau_s$  and  $\tau_m$ .

Many studies of heterogeneity examine the stability of the synchronous or near-synchronous solution when the intrinsic frequencies of the cells are different. In our case, we can parallel this idea by varying the position of the fixed points on the right branches for each cell. This can be achieved by varying various parameters in the equations such as  $I_{ext}$  and  $g_L$ ; see the Appendix. If the parameters  $I_{ext}$  and  $g_L$  are varied between cells, each neuron follows different cubic

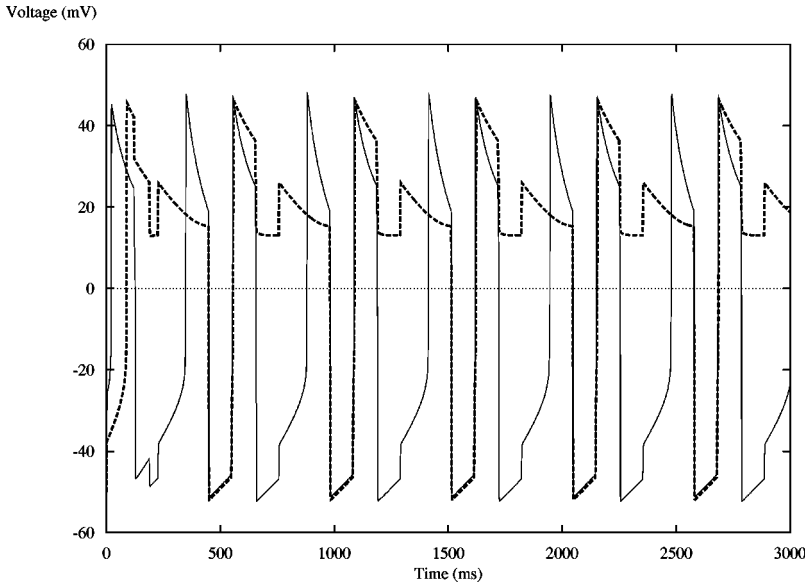


FIG. 10. A 2-to-1 oscillation. Initial conditions and parameter values are the same as in Fig. 9 except that  $\tau=100$ , and for the slower cell  $\tau_R=3$ .

nullclines in the phase plane. However, synchrony can still be stable in these cases if, as in the homogeneous case, both cells jump down at the same time. By choosing a sufficiently large delay, so that both cells can rise above their respective  $RK_2$ 's, this can be achieved. We varied the value of  $I_{ext}$  by up to 20% between cells and still observed stable synchronous orbits (simulations not shown). Similarly, the synchronous solution persisted in the presence of up to 20% heterogeneity in the parameter  $g_L$  between cells. Undoubtedly, the synchronous solution would be persistent to heterogeneity in other sets of parameters.

Varying  $\tau_R$  between cells changes the rate at which the neurons travel on the right branches of the cubic nullcline. By increasing  $\tau_R$  for a particular cell, it will move slower on the right branch than the other cell. Consequently,  $\tau_*$  and  $\tau^*$  will be greater for the cell with the larger  $\tau_R$ . So, again, if the delay is large enough so that both cells are above  $RK_2$  when the second inhibition is felt, the cells will experience time compression during left jumps. Another interesting phenomenon observed while varying  $\tau_R$  is a so-called 2-to-1 oscillation in which one cell oscillates twice while the other cell only oscillates once; see Fig. 10. This is seen by choosing  $\tau_R$  sufficiently large for one cell, as compared to the other cell's  $\tau_R$ . The fast cell will rise above  $RK_2$  before the second inhibition is felt, while the slow cell will become trapped by  $p_2$ . The fast cell then proceeds to jump left, travel down the left branch of  $C_2$ , and then jump right onto the right branch of  $C_1$ . The slow cell will have been released from inhibition and will be on the right branch of  $C_1$  too. The fast cell then catches up to the slow cell and both cells will jump down to the left branch of  $C_2$  when the mutual and self inhibition is felt. Now, both cells will travel down that right branch and eventually jump to the right branch of  $C_0$  when the inhibitions turn off. Again, the slow cell will not be able to rise above  $RK_2$ , while the fast cell will. The process repeats. Notice the fast cell has fired twice and the slow cell has fired once. By making the slower cell even slower, we can obtain  $n$ -to-1 solutions for any  $n$  (simulations not shown). However, if the slow cell is too slow, then it be-

comes permanently trapped in a neighborhood of  $p_2$  and never oscillates, while the faster cell continues to rhythmically fire.

Interesting behavior can also occur without heterogeneity. By making  $\tau_L$  smaller than in the simulations for Fig. 9, in this case  $\tau_L=\tau_R=1$ , synchronous cells can be made to oscillate for a finite number of times before settling into an on-state; see Fig. 11. By selecting an appropriate delay, we can make the cell oscillate for any desired number of times before moving to the on-state. This phenomenon can be explained as follows. The cells start synchronously at  $LK_0$ . The delay is large enough so the cells rise above  $RK_2$  and can jump down freely when the inhibitions turn on. We know that the cells will travel down the left branch of  $C_2$  for a time  $\tau$ , during which they surpass  $LK_0$  if  $\tau$  is large enough. They then jump to the right branch of  $C_0$  and travel up for another time  $\tau$  before the inhibitions are felt again. How far they travel up the right branch depends on how low the cell traveled on the left branch, which in turn depends on the delay time (which we assumed was large enough for the cells to initially rise above  $RK_2$ ). Different delays correspond to different times that the cells spend on the left and right branches of the cubics. If the delay isn't sufficiently large, the cells will become trapped by  $p_2$  when the jump down. If the delay is sufficiently large, the cells will jump left and repeat the process. Some delays cause the cells to oscillate a few times, but each time the cells make a circuit, the height that the cells reach on the right branch of  $C_0$  decreases. Eventually, the cells do not rise above  $RK_2$  and they become trapped in the on-state. This behavior is observed for an interval of these delays.

## V. DISCUSSION

In this paper, we have shown that the length of the synaptic delay is an important parameter to consider when analyzing the dynamics of inhibitory neurons. Its size determines which type of solutions can be stable. An important factor in this determination is the use of self-inhibition

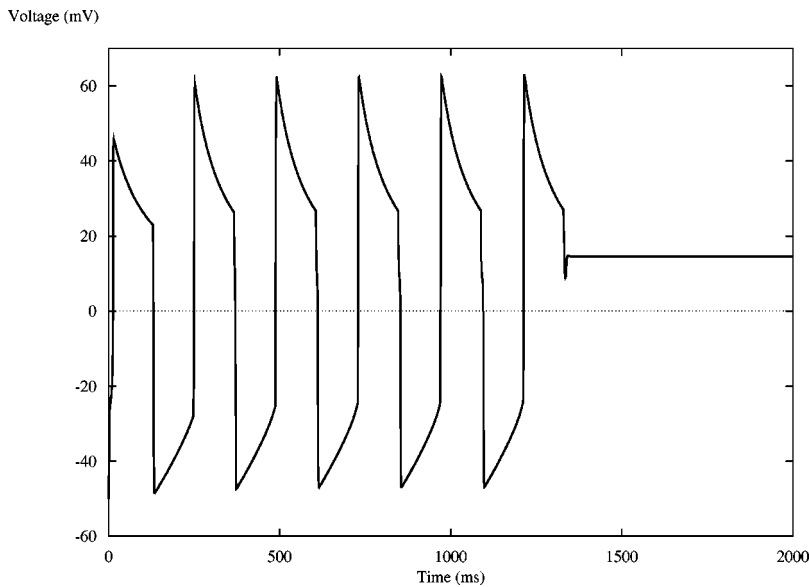


FIG. 11. Synchronous, transient oscillations before the cells settle into an on-state. Parameter values are the same as in Fig. 9 except that  $g_{syn} = 0.15$ ,  $\tau_L = 1$ , and  $\tau = 117.25$ . For suitably chosen values of the delay, the cells can be made to oscillate any finite number of times before moving to the on-state.

within the network. The main advantage that self-inhibition provides is that it allows the cells to feel the same synaptic current at all moments in time. In particular, for the approach to the synchronous solution, it allows cells to jump down from the active phase at the same time. Without self-inhibition in our model, the synchronous solution would be unstable.

Self-inhibition has been considered in other neuronal modeling studies, often in the context of obtaining simplified models of large networks of mutually coupled spiking neurons [5,17]. These studies report that the synchronous solution is stable but require the decay rate of inhibition to be slow. The reason that we do not require slow inhibition is that self-inhibition acts differently for bursting neurons than for spiking neurons. In our case, the self-inhibition acts in the active phase and allows the cells to jump down to the silent state at the same time, creating time compression between cells across the down jump. In the spiking neuron case, the active state of the neuron is ignored and the effect of the self-inhibition is felt when the cell is already back in the silent state. Thus these studies require the slow inhibition to synchronize the cells and do not really need self-inhibition for stability of the synchronous solution. For bursting neurons, self-inhibition also acts differently than mutual inhibition. Mutually coupled bursting cells without self-inhibition also require additional slow currents for synchronization because the cells need not jump down to the silent state at the same time thereby precluding the possibility of time compression on the down jump. Finally, we note that self-inhibition in our model plays little role in the on-state solution and is not crucial for establishing the existence and stability of the antiphase solution. It does, however, determine where in phase space the antiphase solution lies.

The model that we presented also yields stable synchrony in the presence of heterogeneities, both in terms of synaptic and intrinsic parameters. This is in slight contrast to the results of Refs. [5,17], where heterogeneities in intrinsic parameters together with stronger inhibition tend to desynchronize solutions, even in the presence of self-inhibition. In our

model, the compression across the down jump is enhanced due to the existence of the fixed points on the right branch of the cubics. This compression is large enough to overcome the effects of mild heterogeneities. The cells may not jump up to the active state at the same time, but, due to the self-inhibition, will always jump down to the silent state at the same time provided that the delay is sufficiently long. We reiterate that the existence of the fixed points is not critical for stability of intermediate delay synchrony. The fixed points simply expand the range of delays over which synchrony can be achieved.

The role of synaptic delays in modulating the stability of the synchronous solution for networks of coupled cortical excitatory cells has been considered in Ref. [18]. They found that networks with short delays tend to synchronize whereas those with long delays tend to desynchronize. Perhaps not surprisingly, our results are the opposite. However, there are regions of the brain where synchrony is observed between excitatory cells that are anatomically quite far apart such as with pyramidal cells in the hippocampus. Between such cells there are presumably very long synaptic delays. Thus it may be unlikely that this synchrony results from long-range excitation. Our results suggest that networks of interneurons can synchronize over long distances and that the synchrony observed in the pyramidal cell layer may be a reflection of synchrony in the interneuron network. Ermentrout and Kopell showed that long-range synchrony can occur if certain networks of interneurons exhibit spike doublets, where each interneuron fires two spikes in a very short time followed by a longer interdoublet interval. They concluded that the synchrony was induced not by the doublet, but by the fact that each spike in the doublet was produced by a different source of excitation; one coming from a nearby pyramidal cell (with no delay) and the other coming from a far off pyramidal cell (with long delay). While we are not working with a model that has such fine structure to capture doublets, nor are we including excitatory cells, our paper interestingly has one parallel to the work of Ermentrout and Kopell in the following sense: their synchrony requires input from two sources, a

local pyramidal cell and a distant one. Our synchrony also requires input from two sources, local (self-) inhibition and distant (mutual) inhibition. Finally, we note that the previous studies of synchrony between mutually coupled inhibitory cells require two slow currents for stability. It remains to be seen if a minimal network can achieve stable synchrony in the presence of only one synchronizing input or slow current.

#### ACKNOWLEDGMENTS

The authors thank Farzan Nadim for helpful insights and discussions regarding this work. The work of both authors was supported, in part, by grants from the National Science Foundation (DMS-9973230) and by the New Jersey Institute of Technology (421540).

#### APPENDIX: FULL EQUATIONS AND SIMULATION VALUES

The equations used in our simulations are based on the Morris-Lecar model [16]. Parameters that were fixed during the simulations are given below.

$$\begin{aligned} \epsilon \frac{dv_i}{dt} &= I_{ext} - g_l[v_i - E_l] - g_K w_i[v_i - E_K] - g_{Ca} m_\infty(v_i) \\ &\quad \times [v_i - E_{Ca}] - g_{syn} s_i(t - \tau)[v_i - E_{syn}] \\ &\quad - g_{syn} s_j(t - \tau)[v_i - E_{syn}] \\ \frac{dw_i}{dt} &= [w_\infty(v_i) - w_i] / \tau_\infty(v_i), \end{aligned} \quad (A1)$$

$$\epsilon \frac{ds_i}{dt} = \alpha[1 - s_i]H(v_i - v_{th}) - \beta s_i H(v_{th} - v_i),$$

$$\epsilon \frac{ds_j}{dt} = \alpha[1 - s_j]H(v_j - v_{th}) - \beta s_j H(v_{th} - v_j)$$

and

$$\begin{aligned} m_\infty(v_i) &= 0.5 \left[ 1 + \tanh\left(\frac{v_i - mh}{mst}\right) \right], \\ w_\infty(v_i) &= 0.5 \left[ 1 + \tanh\left(\frac{v_i - wh}{wst}\right) \right], \end{aligned} \quad (A2)$$

where  $i \neq j$ .

$\tau_\infty(v_i)$  was defined previously as a Heaviside function. However, in the simulations, the Heaviside function was replaced with a tanh function.

$$\tau_\infty(v_i) = 0.5[1 + \tanh(20[v_i - v_{th}])][\tau_R - \tau_L] + \tau_L. \quad (A3)$$

The values of the parameters used in the simulations are  $I_{ext} = 50$ ,  $g_l = 0.5$ ,  $E_l = -50$ ,  $g_K = 2$ ,  $E_K = -70$ ,  $g_{Ca} = 1.9$ ,  $E_{Ca} = 100$ ,  $\epsilon = 0.01$ ,  $g_{syn} = 0.25$ ,  $E_{syn} = -100$ ,  $\alpha = 20$ ,  $\beta = 20$ ,  $mh = 1$ ,  $mst = 14.5$ ,  $wh = 12$ ,  $wst = 5$ ,  $v_{th} = 0$ ,  $\tau_L = 2$ , and  $\tau_R = 1$ .

- 
- [1] G. Ermentrout and N. Kopell, Proc. Natl. Acad. Sci. U.S.A. **95**, 1259 (1998).  
 [2] J. Rubin and D. Terman, Neural Comput. **12**, 597 (2000).  
 [3] D. Terman, A. Bose, and N. Kopell, Proc. Natl. Acad. Sci. U.S.A. **93**, 15417 (1996).  
 [4] A. Bose, V. Booth, and M. Recce, J. Comput. Neurosci. **9**, 5 (2000).  
 [5] C. Chow, Physica D **118**, 343 (1998).  
 [6] W. Gerstner, J. van Hemmen, and J. Cowan, Neural Comput. **8**, 837 (1996).  
 [7] D. Terman, N. Kopell, and A. Bose, Physica D **117**, 241 (1998).  
 [8] C. van Vreeswijk, L. Abbott, and G. Ermentrout, J. Comput. Neurosci. **1**, 313 (1994).  
 [9] T. Gilbertson and H. Zhang, J. Gen. Physiol. **111**, 667 (1998).  
 [10] M. Kloub, G. Heck, and J. DeSimone, J. Neurophysiol. **79**, 911 (1998).  
 [11] D. Osorio, Visual Neurosci. **7**, 345 (1991).  
 [12] L. Palmer, H. Sackin, and G. Frindt, J. Physiol. (London) **509**, 151 (1998).  
 [13] F. Nadim, Y. Manor, M. Nussbaum, and E. Marder, J. Neurosci. **19**, 5053 (1998).  
 [14] E. Mishchenko and N. Rozov, *Differential Equations with a Small Parameter and Relaxation Oscillations* (Plenum Press, New York, 1980).  
 [15] D. Somers and N. Kopell, Biol. Cybern. **68**, 393 (1993).  
 [16] C. Morris and H. Lecar, Biophys. J. **35**, 193 (1981).  
 [17] J. White, C. Chow, J. Ritt, C. Soto-Trevino, and N. Kopell, J. Comput. Neurosci. **5**, 5 (1998).  
 [18] S. Crook, G. Ermentrout, M. Vanier, and J. Bower, J. Comput. Neurosci. **4**, 161 (1997).